Development and Deployment of a UAV-Borne Gas Capture System for Fumarole Sampling

Matthew Anderson *, Spencer Backus[†], Ery Hughes[‡], Aaron Curtis[§], Soon-Jo Chung[¶], and Edward M. Stolper[‖]
California Institute of Technology, Pasadena, CA, 91125
Jet Propulsion Laboratory, Pasadena, CA, 91109

Volcanoes are one of the great forces of the natural world. The gases they release can reveal information about the world below us, from the structure of the planet, to the risk of an imminent eruption. Capturing volcanic gases, however, is often difficult and extremely dangerous - high temperatures, steep terrain and remoteness all make collecting samples a challenging endeavour. Unoccupied Aerial Vehicles (UAVs) can help reduce the risks and difficulties of measuring and sampling these gases, enabling studies of volcanic systems that were otherwise inaccessible. This paper presents the first known effort to design, develop and field test a UAV-borne Gas Capture System (UGCS) for volcanic fumarole sampling. This work includes the development of a sampling probe deployment mechanism, sample canister selection, payload-to-UAV interfacing, and a light-weight visual/thermal camera package. Operationally, the intricacies of placing a sample probe into a small fumarole opening are examined, as are the hazards of flying a UAV with a suspended load. Finally, the results of both lab testing and field testing at the volcanic fumaroles near Mammoth Lakes, CA, are presented.

I. Introduction

A. The Importance of Measuring Volcanic Emissions

Volcanoes release gases and particulates into the atmosphere that influence the local and global climate over periods of months to millions of years. Volcanism is a major source of non-anthropogenic CO_2 and other greenhouse gases, and has been one of the dominant driving forces behind climate change on geological timescales [1–3]. Estimates of the contributions of volcanic CO_2 emissions vary significantly [4], in part due to our understanding of volcanic systems being dominated by a few accessible volcanoes that are unlikely to be globally representative [5]. In addition to CO_2, volcanic emissions include sulphur (which both generates volcanic smog and ozone-depleting sulphate aerosols) and halogens (both a health hazard and depleter of ozone) [6]. Additionally, violent eruptions, often unforeseen, can cause severe damage to life, property and the surrounding ecosystems in a way few other natural events can. Sampling of the gases emitted by volcanoes can be used to predict the shift from a quiescent periods to imminent explosive eruptions [7, 8].

Around volcanoes, gases are emitted actively during eruptions and passively during quiescent periods in plumes, fumaroles, springs, and diffusively through surrounding lakes and terrain [9]. The mechanism of gas emission affects how contaminated the sample is compared to the gas released in equilibrium with the magma at depth. Plume gases interact extensively with the atmosphere, whilst springs and diffusive ground and lake emissions have extended time interacting with the sub-surface, hence, these gases are contaminated by the time they can be sampled. A fumarole is an opening that emits gases at the Earth's surface. They can occur as cracks or fissures (cm to m in size) in volcanic vents, in the surrounding regions, or even on active lava flows. High-temperature fumaroles have the shortest connection path to the gas in equilibrium with the magma, limiting interaction and contamination prior to emission at the surface, and therefore provide the best representation of magmatic gas. Hence, samples from high-temperature fumaroles are needed to accurately estimate the magmatic gas composition and understand changes in the magmatic system at depth.

---

*Postdoctoral Scholar in Aerospace, 1200 E California Blvd

[†]Robotics Engineer, Jet Propulsion Laboratory, California Institute of Technology, 4800 Oak Grove Drive

[‡]Postdoctoral Scholar Research Associate in Geology, 1200 E California Blvd

[§]Software Systems Engineer, Jet Propulsion Laboratory, California Institute of Technology, 4800 Oak Grove Drive

[¶]Bren Professor of Aerospace and Jet Propulsion Laboratory Research Scientist; 1200 E California Blvd, AIAA Associate Fellow

[‖]Robert Andrews Millikan Professor of Geology, 1200 E California Blvd

B. UAV Operations around Volcanic Systems

In the past decade, UAVs have become an enabling technology in the field of volcanology and several previous works have used UAVs to study volcanic plume systems (a review paper summarising these efforts and UAVs for volcanic studies in general is available in [10]). *In situ* measurements of volcanic plumes with UAVs was first demonstrated in 2007 with flights over La Fossa crater (Italy) using a small helicopter carrying a 3 kg payload for measuring CO_2/SO_2 ratios and SO_2 flux [11]. This work showed the great potential for using UAVs for such tasks due to their high level of stability, slower flight speeds, and inherent safety of not placing a pilot at risk. Mori et al. [12] studied the plume of Mt Ontake (Japan) after the 2014 eruption using UAVs and multiple payloads including a 1.3 kg gas analyser (SO_2, H_2S, CO_2 and H_2O) and a 0.8 kg camera package (RGB and long-wave thermal). D'Arcy et al. [8] studied Masaya (Nicaragua) and Turrialba (Costa Rica) with a 1.5 kg gas sensor (CO_2, SO_2 and H_2S concentration and SO_2 flux) and a 0.95 kg gas spectrometer. Several aircraft types including fixed-wing, large octocopters and small quadrotors were used to fly around the volcano and the different vehicles were shown to excel at flying different mission types. Rüediger et al. [13] successfully tested at Stromboli (Italy), Turrialba (Costa Rica) and Masaya (Nicaragua) volcanoes carrying CO_2 and SO_2 sensors and a miniature UV spectrometer. Missions were flown manually and the real-time sensor feedback was used to help the pilot guide the aircraft into the most concentrated region of the plume. The dense plumes caused interference in the remote control connection between the pilot and the aircraft, and the GPS automated return function was required to successfully recover the aircraft. Liu et al. [14] flew over Volcán de Fuego (Guatemala) and compared ground-based gas compositions with those measured on-board the UAV, showing good agreement between the two measurement methods.

The ability to fly through plumes was further extended by Schellenberg et al. [15] who developed an on-board, real-time trajectory planner to allow their UAV to adapt to the volatile and rapidly-changing atmospheric conditions around volcanoes. This capability allowed the vehicle to operate over 9 km away from and 3 km above its launch location and was proven to generate efficient, safe flight plans over Volcán de Fuego (Guatemala). Wood et al. [16] have also completed Beyond Visual Line-of-Sight (BVLoS) operations, providing a detailed review of the challenges of operating at long ranges in the volcanic plumes of Manam (Papua New Guinea), and even include the events that led to the loss of their aircraft.

Typically, gas studies with UAVs measure the gas *in situ* using light-weight sensors that are limited in type and accuracy when compared to those that are available in a ground-based laboratory. Li et al. [17] developed a UAV-borne gas capture system (UGCS) designed for collecting samples for later analysis. This work, however, was focussed on general atmospheric measurements rather than extreme environments. The system collects the gas samples using a probe mounted 1.2 m above the UAV where the propeller in-wash velocity was shown to be minimal using CFD analysis. Experimental testing of Li's UGCS showed good agreement between ground-based measurements and *in situ* UAV measurements of the CO_2 and particulate concentrations, validating the concept of collecting gases using a UAV-borne system for later lab-based analysis.

C. Paper Overview

This work proposes an enabling technology for studying previously inaccessible volcanic vents and presents the design and testing of a light-weight, UAV-borne gas capture system that is capable of collecting and returning gas samples from the opening of a fumarole. The presented system consists of a heat-resistant, deployable sampling inlet, a pump, valve manifold, and two gas sample canisters used to collect and store multiple gas samples per flight. Additionally, gas sensors and cameras are used to identify and perform preliminary *in situ* measurements of candidate fumaroles. The work presented here is unique as it is the only known effort to develop a UAV-borne system to directly capture gasses that are emitted from typically inaccessible, high-temperature fumarole vents in a similar way to how scientists collect samples by hand at accessible fumaroles.

This paper first describes the UAV platform used, followed by a description of the spool mechanism and gas capture modules used to capture and store the fumarole gases on-board the UAV. The in-development autonomy package mounted to the UAV is then presented and the overall network architecture used to communicate with the UAV and control the payload is shown. The results of bench-testing and lab-based flight testing (both indoors and outdoors) is then presented, showing the ability of the system to capture and store gases while hovering, as well as sharing some lessons learnt. Finally, this work culminates in a field deployment to the fumaroles near Mammoth Lakes, CA, and suggests some future directions of development for similar systems.

II. System Design

A. UAV Overview

Volcano Drone is a light-weight, custom-framed carbon-fibre quadrotor developed in conjunction with the Center for Autonomous Systems and Technologies (CAST), Caltech (Figure 1). It can carry approximately 1.5 kg of payload for around 15 minutes with two 6S 6000 mAh batteries in parallel for a total vehicle weight (including payload) of 4.5 kg. A Pixhawk 4 running ArduCopter 4.0.5 [18] controls *Volcano Drone* and a Here+ RTK GPS and HereFlow optical flow sensor provide local and global position state feedback. The motors are controlled via telemetry-enabled ESCs (via Dshot), allowing the propeller speeds and individual motor currents to be monitored throughout the flight. Manual control is though a telemetry-enabled Spektrum receiver which allows the pilot to fly either in fully-manual modes (such as Stabilise Mode) or with position hold assistance from the autopilot (such as Loiter Mode). The receiver also monitors the battery voltage, giving the pilot an independent battery status reading to help ensure the battery does not unexpectedly run out. Finally, high-brightness LEDs mounted below the motor arms aid in visibility and attitude determination for the pilot.
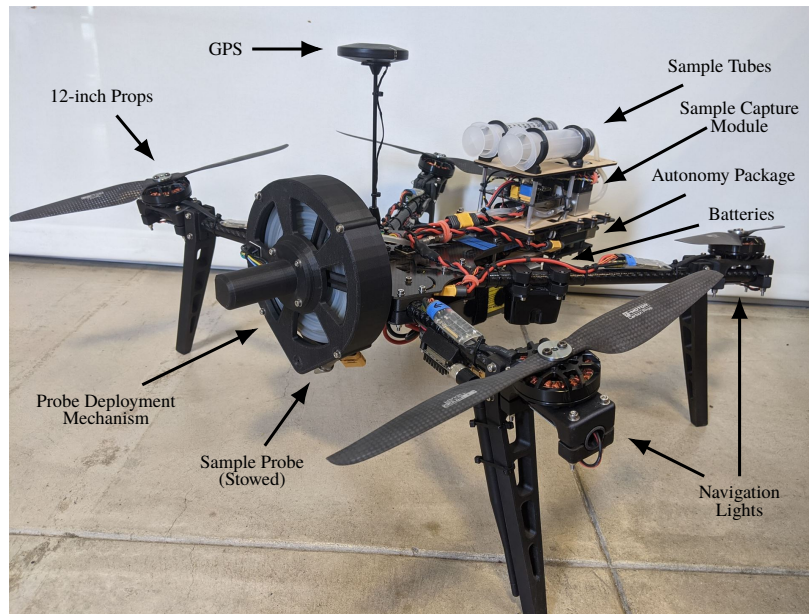

Fig. 1 *Volcano Drone* **with UAV-Borne Gas Capture System Mounted**

Volcano Drone has a large amount of excess thrust to ensure it can operate in the lower-density air found at high elevations. Additional control authority in yaw is generated by canting the motors 12 deg inwards, enabling flight in the more turbulent air that is expected around volcanoes. The flat top enables payloads to be added and removed easily as required, and the battery can shift to ensure a balanced centre-of-gravity.

B. UAV-borne Gas Capture System Overview

The UAV-borne Gas Capture System (UGCS) features two main components, the Probe Deployment Mechanism and the Sample Capture Module (Figure 2), and has a mass of 1.5 kg. Additionally, an in-development autonomy package is mounted at the bottom rear of the UAV (Figure 1) that will help future missions autonomously locate, target and sample fumaroles using real-time mission planning algorithms.

1. Probe Deployment Mechanism

Mounted at the front of the UAV, the Probe Deployment Mechanism (Figures 1 and 3) can deploy and retract up to 2 m of tubing to sample gases from the fumarole below. Although the temperature inside the fumarole can be many hundreds of degrees Celsius (for example, 100 °C at Salton Sea, CA [19], 562 °C at Kīlauea, HI [20], and 650 °C at Mutnovsky, Russia [21]), the heat dissipates quickly as the gases mix with the atmosphere [22]. The long, extendable
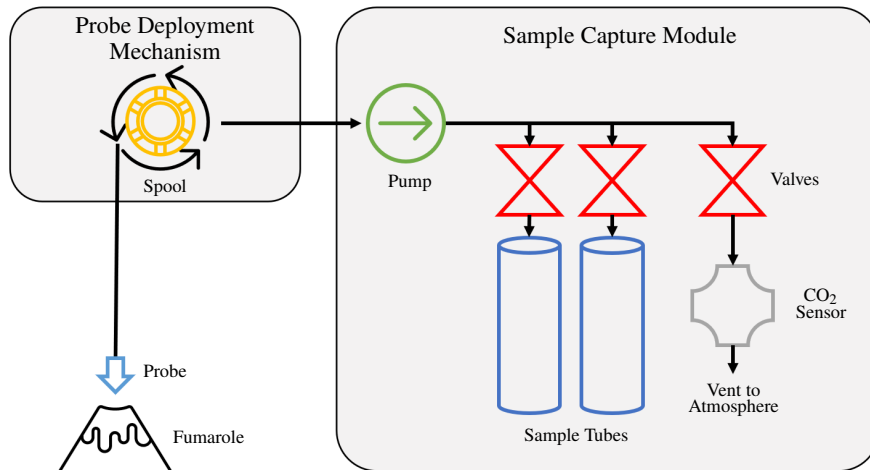
Fig. 2   Schematic of the UAV-Borne Gas Capture System

tube enables the UAV to remain safely above the high temperature and caustic gas concentrations that would otherwise damage or destabilise the aircraft. The amount of tube deployed is calculated from an encoder on the spool shaft and is controlled using a brushed motor controller which has built-in torque feedback to prevent the system from over-retracting the tube and damaging the spool mechanism.
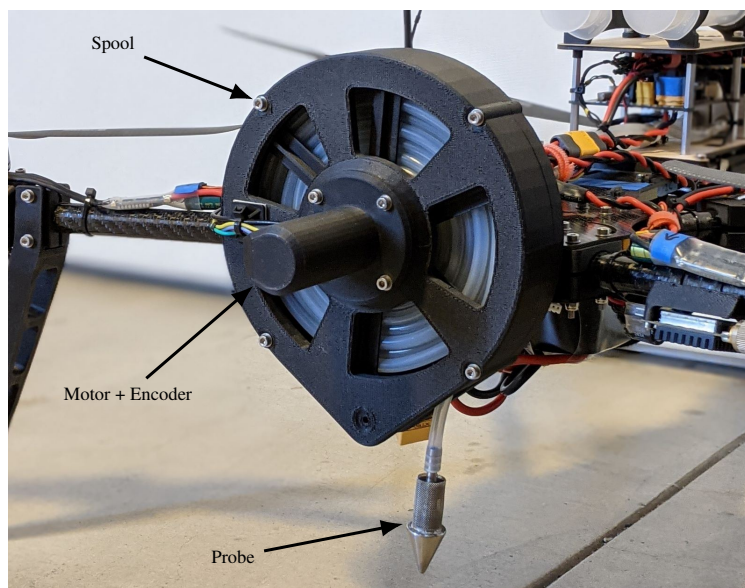

Fig. 3   The Probe Deployment Mechanism with the Sample Probe Partially Extended

The tube is made from silicone, which is flexible and resistant to high temperatures. Silicone tubing is available in many different hardnesses and testing revealed 3 mm, 50 duro tube gave a good balance between flexibility to enable winding and stiffness to avoid kinking. The probe end used is a Gas Vapor Tip and Screen probe from EnviroSupply and has a screen to prevent larger particles from entering the tubing and clogging the pump and valves. The relatively large weight of the probe end helps to draw the tubing out of the spool and drops the sampling end straight down with minimal bowing.

2. Sample Capture Module

The Sample Capture Module containing the payload control, sample canisters and pump is located at the rear of the aircraft (Figures 1 and 4). The pump is used to draw air in from the fumarole, through the tubes and into the rest of the system. The pump is capable of pressurising the gas above atmospheric pressure, allowing the sample canisters to be pressurised such that any leakages flow from the sample canisters to the atmosphere, keeping the samples as uncontaminated as possible. The flow is controlled to each of the sample canisters individually using electric solenoid valves, enabling samples from different fumaroles to be taken in a single flight. The length of tube between the valves and canisters was kept as short as possible to minimise the amount of 'dead air' entering the canisters. Future iterations of the system will enable the pump to be reversed so this volume can be evacuated prior to flight, effectively preventing any 'dead air' fouling the sample. Finally, an additional valve is used to control the flow to the atmosphere, preventing air from being back-drawn into the system.
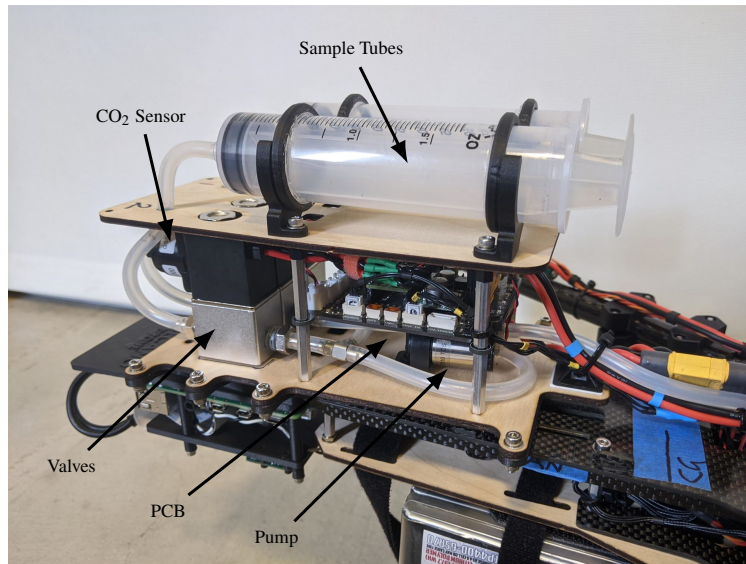

Fig. 4   Sample Capture Module

Though the sample capture module is designed to capture gas for laboratory analysis, it is important from an operations perspective to be able to detect a 'tracer' gas in real-time to determine if the probe is correctly placed inside the fumarole. CO_2 was chosen as the tracer gas as it is present in quantities significantly above atmospheric in fumaroles [19, 23, 24], and the sensors are much cheaper and lighter-weight than those required for many other gases. The CO_2 sensor chosen was the SprintIR-W CO_2 sensor due to its low weight and power requirements. The SprintIR is available in many different sensing ranges (5 %, 20 %, 60 % and 100 %) that all use the same package, meaning the sensor can be tailored for the particular fumarole system without needing to redesign the system or software. To ensure the CO_2 levels sensed in real-time are those that will be sampled into the canisters, the CO_2 sensor is placed at the vent-to-atmosphere downstream of the valves (Figure 2). Testing showed that placing the CO_2 sensor downstream of the valve to atmosphere was important as the sensor was not able to hold pressure well and typically leaked.

The UGCS is controlled using a Teensy 4.0 mounted on a custom PCB which contains all the required components for voltage regulation, solenoid control, pump power and sensor interfacing. The Teensy is programmed using Arduino and is interfaced with the flight controller via a UART connection to provide remote communications (Section II.B.5). Where possible, COTS components were used to simplify assembly, and the whole system is powered directly from the UAV battery.

3. Gas Capture Canisters

The sample canisters (Figure 5) must be both light-weight and have a good long-term retention rate, especially if the gases of interest (such as hydrogen and helium) can leak through most materials. For initial testing, standard 50 ml syringes were used as they are easily filled and evacuated, and the rigidity makes securely mounting them to the UAV simple. Sealing the syringes well, however, is difficult and hence the leak rate is high, making them ill-suited

for research missions. Pre-evacuated IsoTubes were floated as a possible replacement as they are light-weight, rigid (making them easy to mount) and easy to interface with (via the Schrader valves at each end). IsoTubes however are not designed for gases containing H_2S [25], making them unsuitable for use at many volcanic fumaroles.

Fig. 5   A Selection of the Sample Canisters. Left-to-right: Syringe (50 ml), IsoTube (100 ml), Tedlar Bag (500 ml), Multi-Layer Foil Bag (1 000 ml).

For fumaroles with high H_2S concentrations, Tedlar bags and multi-layer foil bags provide a light-weight, chemically inert solution. However, these sampling bags are more difficult to securely mount to the UAV than rigid options (as they change volume with the amount of gas contained), and have a higher leak rate than metal or glass sample tubes [26]. To overcome the leak rate issue, the gases will be captured using the multi-layer foil bags and then transferred to heavier, more suitable long-term storage canisters upon landing, minimising the losses before the samples reach the laboratory. Furthermore, as the time between capture and transfer is known, the losses can be modelled and corrections applied to give an accurate reading of the originally captured gas.

4. Higher-Level Autonomy Package

Although the work presented in this paper is manually piloted, *Volcano Drone* is designed to operate Beyond Visual Line-of-Sight at locations that are inaccessible to humans. As such, a significant level of autonomy will be required to path plan, locate, target and sample the fumaroles without any direct involvement from operators on the ground. To support this work into the future, an autonomy package was developed that features a FLIR Lepton v3.5 long-wave thermal imager, RPi Camera v2 (visible spectrum), and a Raspberry Pi 4 (2 GB) (Figure 6).
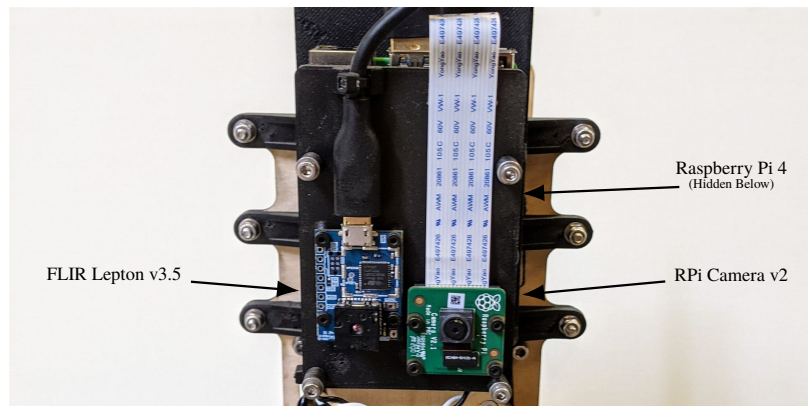

Fig. 6   Autonomy Package Mounted to the Bottom of *Volcano Drone*

Fumaroles may not be very distinct in the visible spectrum of light (especially when viewed from above), and often look very similar to the surroundings. As the FLIR Lepton measures long-wave IR (emitted heat), hot-spots (and heat differences in general) are easily identified, meaning the heat signatures of the fumaroles can be used to identify and

track potential locations of interest from a distance. Furthermore, the FLIR Lepton provides radiometric measurements for each pixel, allowing the approximate temperature of the fumarole to be measured. The RPi Camera complements the information provided by the FLIR by capturing visible light images of the fumarole that are easier for humans to interpret. Furthermore, the images can be used to produce maps which can be used to monitoring how the environment is changing (such as in [27]).

The Raspberry Pi 4 (RPi) was chosen as the companion computer as it features sufficient computational power for processing the low-resolution (160 px × 120 px) FLIR images in real-time at a low weight and power. The RPi is interfaced to the flight controller using ROS and mavros (via a UART mavlink connection), enabling information such as position, payload control, and guidance commands to be shared between the two. Furthermore, ROS handles all the logging (including from the cameras), enabling the imagery and collected samples to be geo-tagged in post-processing.

5. Network and Operator Interface

The payload is controlled by a Teensy 4.0 that communicates with the flight controller via a UART mavlink connection [28]. A custom library* was developed to handle this interfacing, making it simple to reuse the code on other projects that require similar capabilities. This mavlink connection allows the flight controller to share information such as position, altitude, and commands with the payload, enabling it to interact with and respond to the state of the aircraft. Payload control is via spare RC Out channels from the flight controller, which reads directly from the mavlink packets, reducing the amount of wiring required. Controlling the payload via RC Out channels (rather than through custom commands) means the flight controller firmware and mavlink dialect remain standard, greatly reducing the complexity and development time required. The payload uses information from the UAV to deploy the appropriate length of tube based upon the altitude at the time, and also features 'safe-gaurds' that retract the spool if the payload detects the pilot is moving away from the fumarole but has forgotten to retract the probe. The measured CO_2 concentrations and state of the payload (such as sampling state and remaining sample tubes) are communicated to the user via mavlink message packets.
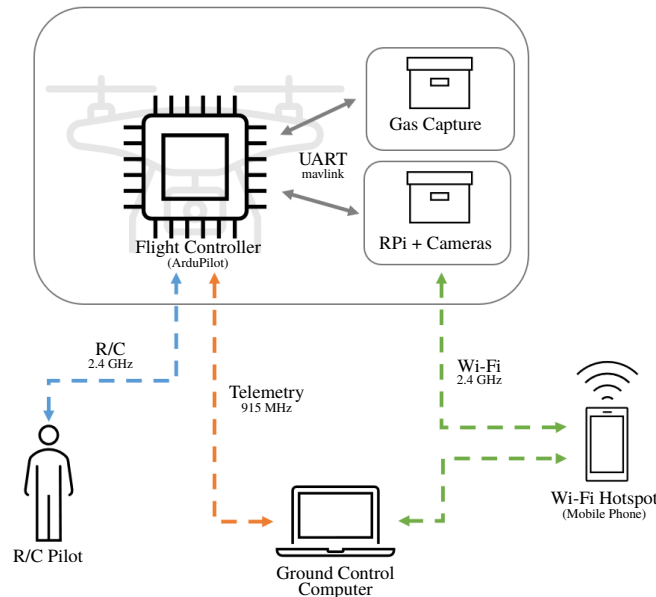

Fig. 7   Communications Setup. Solid lines are wired links, dashed lines are wireless links.

The flight controller uses a long-range, 915 MHz mavlink telemetry link (RFD900x radios) to connect to the ground station (Figure 7). The ground station runs Mission Planner and is capable of remotely monitoring and flying the UAV, as well as controlling the payload through the Servo/Relay control tab to manually set the outputs of the payload control channels. The payload automatically detects and assigns itself the same identification number as the UAV to help with automatic packet routing, and the source of the packets is distinguished by using differing component IDs for the UAV

---

*The Arduino-mavlink library was written based on the excellent tutorial available at `https://discuss.ardupilot.org/t/mavlink-and-arduino-step-by-step/` and the pre-compiled headers from `https://github.com/mavlink/c_library_v2`

and payload. By piggybacking the payload telemetry link onto the already existing telemetry link of the aircraft, the system is significantly simplified, both in hardware (as no additional hardware is needed) and frequency management (fewer components transmitting on potentially the same bands).

A 2.4 GHz Wi-Fi connection is used to interface the companion computer to the ground station via ssh. A mobile phone hotspot is used as the router, reducing the extra equipment required to operate the aircraft, a useful aspect when the launch site may be a long distance on foot from a vehicle-accessible road. The mobile phone hotspot also enables internet connectivity in the field where celluar service is available. Finally, avahi is used to address the RPi by hostname (rather than IP address) as mobile hotspots typically have a limited ability to configure the router, meaning the aircraft never gets 'lost' on the network.

III. Bench Testing

A. Pump Flow Rate and Purge Time

Before capturing a sample or taking a measurement, the air lines must be purged to clear existing gas out. The time required to purge the air lines can be determined by pumping gases of significantly different (but not necessarily known) CO_2 concentrations through and measuring the gas CO_2 concentration at the vent to atmosphere. In this case, the easiest way of generating the two different CO_2 concentrations was to use fresh air (approx. 0.04 % CO_2, inlet open to atmosphere) and human-exhaled air (approx. 3.8 % CO_2, contained inside a Tedlar bag).
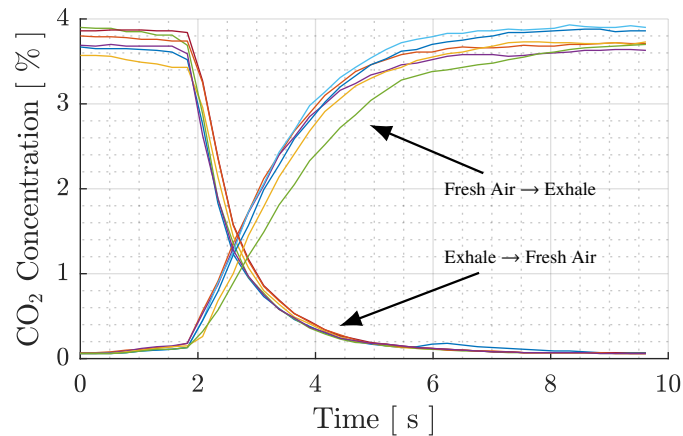

Fig. 8 CO_2 Concentration Detected vs. Pump Time (12 Tests)

Figure 8 shows the measured CO_2 concentration from the on-board CO_2 sensor across 12 tests as a function of time. Little change is seen for the first two seconds of pumping, after which the concentration begins to change quickly and then asymptotically levels off to near-constant after eight seconds. As such, the payload is programmed to purge the air lines for 10 s before reading the CO_2 (or taking a sample), ensuring there is no gas in the line from a previous location. In order to speed up the process of capturing a sample, the payload only purges the lines if the air is older than 20 s, enabling the CO_2 to be read then captured in quick succession without needing to wait for unnecessary purge cycles.

B. Fumarole Simulator Development

A fumarole simulator was developed out of a small, cylindrical plastic container (110 mm diameter, 70 mm high) and was designed to provide a concentrated CO_2 source to practice placing the sample probe with the UAV. Initially, the CO_2 source was provided by a mixture of bicarbonate of soda and vinegar (the classic school volcano experiment), and while this worked well for quick tests, the reaction typically persisted for less than a minute, and hence was too short to enable any useful testing. The CO_2 source was thus replaced with dry ice (frozen CO_2) which proved to be a very effective solution (Figure 9). The dry ice produces CO_2 for a significant amount of time (on the order of hours) and the measured CO_2 in the fumarole simulator was typically >90 % (though at a very slow outgassing rate). Furthermore, the cold temperature of the dry ice produces a distinct temperature marker for the thermal camera, effectively mimicking the temperature difference between the environment and a fumarole.
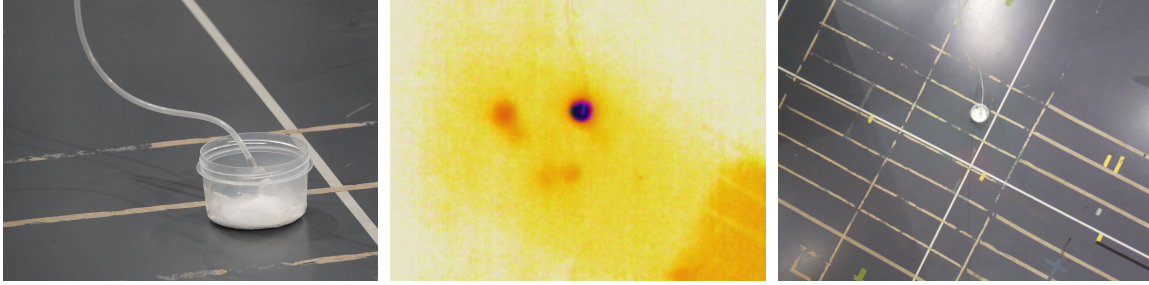
Fig. 9   The Dry Ice Fumarole Simulator (Left) with the Thermal (Centre) and RGB (Right) Imagary Collected While Sampling from the Dry Ice Fumarole at CAST, Caltech. The dark spot in the thermal image corresponds to the current location of the fumarole simulator, while the lighter-coloured dark spots show where the fumarole simulator had previously been placed.

IV. Flight Testing

A. Indoor Testing

1. *Placing the Probe into the Fumarole Simulator*

Indoor flight testing was conducted in the CAST Flying Arena at Caltech. Initial testing of probe deployments were piloted in stabilise mode with the pilot having direct control over the attitude and thrust of the UAV. Maintaining a sufficiently steady hover to drop the probe straight down into the fumarole simulator proved very difficult, with the recirculation effects of flying in an enclosed space and disturbance forces from the probe perturbing the vehicle. This non-steady hover then fed forces back into the probe end, and caused a significant amount of sway that made accurate probe placement almost impossible.

Switching the UAV into a position hold mode was very effective, especially when the optical flow sensor was used to aid the state estimate (positioning was typically held within a sphere of radius 0.1 m). The high rate of the control loops mean that the UAV responds quickly to disturbances and actively corrects the position without over-correcting and exciting the probe sway. Though the probe enters the field-of-view of the optical flow sensor at full extension, no adverse effects on the position tracking were observed.
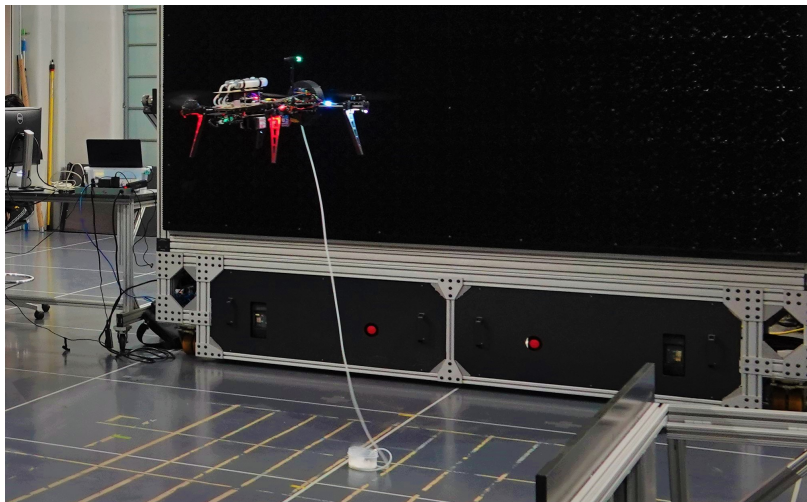

Fig. 10   Testing Spool Deployment and Probe Sway in Wind at CAST, Caltech

Manually controlling the position of the UAV (in Loiter mode) and sinking the probe in the 110 mm diameter hole of the fumarole simulator was difficult, typically taking in the order of 5 minutes (the region of impact when the probe was initially deployed was approximately 300 mm). Though the probe typically drops from the stowed position with little

9

sway, a 'missed attempt' that hits the ground (or manoeuvring to correct the position) causes low amplitude oscillations in the probe position that were approximately twice the size of the fumarole hole. Attempting to time the swaying motion and descend the UAV to sink the probe was also difficult due to the lag between stick input and vehicle descent. With practice the pilot did improve, approximately halving the time taken to correctly place the probe. Techniques such as dragging the probe along the ground into the fumarole hole worked well, though using this technique in the field would require the fumarole be sunken into the ground, and hence would not work for raised features such as gryphons (mud volcanoes), or around features such as salses (mud pots) where the surrounding ground could clog the probe.

The CAST wind-tunnel was then used to qualitatively determine the effect of wind on the probe sway and the ability to place the probe accurately in the presence of wind (Figure 10). Wind speeds up to 5 m/s were trialled, and showed that while the probe itself was not substantially affected by the wind (primarily due to the low cross-sectional area and large weight of the probe end), the wind did degrade the performance of the position hold controller. This added movement of the UAV then fed back into the probe and increased the amount of sway, though not to the point where placing the probe accurately became unmanageable.

2. In-Situ CO_2 Measurements from the Fumarole Simulator

Figure 11 shows the concentration of CO_2 as measured by the UGCS during testing with the dry ice fumarole. Data points were taken before the flight, hovering above the fumarole, hovering 1 m behind the fumarole, upon landing, and 1 min after landing (joined lines represent single flights). While hovering, the downwash from the propellers replaces the air in the fumarole simulator with free air from above, significantly reducing the measured CO_2 concentration from the baseline measurement. Hovering over the fumarole and taking continuous samples showed that it took in the order of 30 s to reach a steady-state CO_2 value (hence why the hovering behind case is lower in CO_2). Mitigation efforts were attempted including placing the probe then manoeuvring the UAV away from the fumarole (approximately 1 m back and 1 m altitude), however the downwash effect was equally large in both cases. Upon landing, the CO_2 concentration recovers slowly, and is based upon the outgassing rate of the source.
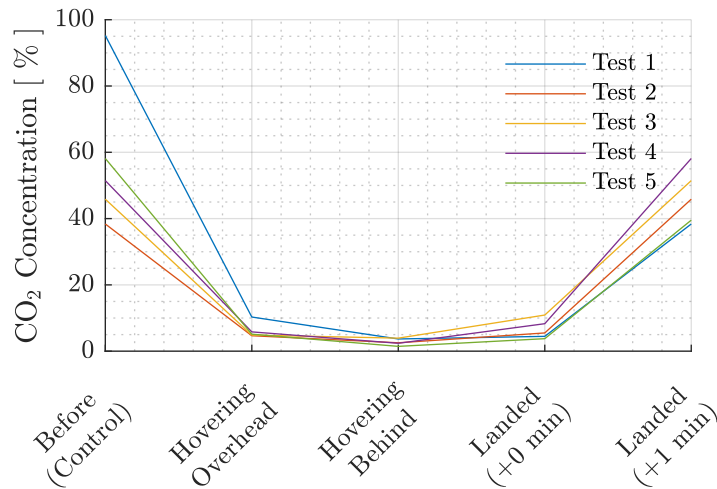

Fig. 11   Concentration of CO_2 as Measured During Testing with the Dry Ice Fumarole. The probe was fixed in the fumarole to remove the requirement of piloting the probe into the fumarole simulator each time, greatly reducing testing time. The initial concentrations of CO_2 are lower after Test 1 as the fumarole simulator did not reach steady-state before the next test was attempted.

This downwash effect is expected to be a function of the height above the fumarole, however it is likely that the tube would need to extend on the order of tens of metres to be long enough to ameliorate the downwash effect. Placing the sample probe on a boom that extends out in front of the UAV would have similar issues of scale as the downwash strikes the ground and flows outwards, and is very noticeable even at 10 m away. Procedurally, the UAV could place the probe in the fumarole, move back, land, wait, and capture the sample. The time to wait would depend upon the outgassing rate of the fumarole (likely unknown *a priori*), though continuously monitoring the readings from the fumarole and waiting for a steady state to be achieved would allow for different outgassing rates to be actively adapted for. This technique

however requires relatively flat and level ground for the UAV to land on, and is unlikely to be the case for many of the inaccessible fumaroles this work is targeted towards.

3. CO_2 Measurements of Captured Gases

Gas samples captured while hovering over the fumarole simulator were stored on-board the UGCS in the 50 ml syringes. These samples were used to determine if the gas captured by the UGCS was representative of the gas as measured from the probe in-flight. The CO_2 concentration (as measured by the *in situ* CO_2 sensor) was recorded as the samples were being captured. The UAV was then landed, and the valves were opened to allow each of 50 ml syringe samples to flow individually out through the CO_2 sensor. The plunger was then used to push the captured gas sample through the CO_2 sensor and the CO_2 measurements were recorded.

Very good agreement was seen between the CO_2 measurements taken in-flight and those measured later from the captured gas samples, with both measurements agreeing to within the noise level of the sensor. The CO_2 concentration as measured from the captured gas sample is expected to be lower (due to the 'dead air' inside the tubes), however this volume is very small compared to the syringe volume, hence the very small difference in CO_2 concentration.

These sample capture tests show that it is possible to capture and store gases in-flight and then transport them back to the ground with minimal fouling of the sample.

B. Outdoor 'Lab' Flight Testing

Outdoor 'lab' flight testing was completed at North Field, Caltech. The larger space and GPS reception allowed for more realistic tests and to practice approaches and departures from the fumarole (rather than starting almost above the fumarole simulator as was done in CAST). Initially, the position estimate was aided only by the GPS, and while the position hold was good, it was only marginally sufficient to minimise the probe sway enough that it was possible to sink the probe into the fumarole simulator. The optical flow sensor was re-enabled to complement the GPS and the higher-accuracy position hold behaviour of the indoor flight testing returned.

Fig. 12   Manoeuvring with the Tether Deployed. The large mass of the probe coupled with the long tube length means the probe lags significantly behind the vehicle and even small manoeuvres at low speeds can introduce significant swinging.

The larger space of North Field enabled larger manoeuvres to be trialed and it was quickly discovered that translations, even at low speeds, caused the probe to lag significantly behind the UAV (Figure 12), which in turn caused large-amplitude swinging of the probe end that took a long time to settle. Furthermore, retracting the spool to stop the swinging and start over proved to be a poor response - conservation of angular momentum means that the swinging increases in amplitude

and frequency as the spool is retracted, and has the potential of swinging the tube and probe through the propeller blades. Dangerous-amplitude swinging during spool retraction was observed for even seemingly low-amplitude initial swinging conditions.

The outdoor lab tests also showed a potential failure case introduced with the automatic spool retraction logic where the spool is automatically retracted if the vehicle is detected leaving the fumarole. As the UAV leaves the fumarole and begins a transit to the next location, the probe is likely to be lagging behind, and retracting the probe at this point, once again, causes large amplitude oscillations that could potentially swing the probe through the propeller blades. Hence, this behaviour was removed as it was deemed safer to fly with the tube extended (and risk it getting caught) than to blindly attempt to retract the tube and risk contact with the propellers.

C. Deployment to the Fumaroles Near Mammoth Lakes, CA

Volcano Drone and the UGCS were field tested at Basalt and Shady Rest Fumaroles near Mammoth Lakes, CA. Both fumaroles are at approximately 2 400 m (7 900 ft.) elevation and were chosen as they are accessible and emit high-temperature gases, enabling for the preliminary testing and verification of the UGCS in a reasonably safe environment.

Fig. 13   A Vent Under a Rock (Left) and Capped Vents (Right) at Basalt Fumarole, Inyo National Forest, CA

Basalt Fumarole (37.644867 N, 118.930352 W) was used as the primary test site as there were many open volcanic vents with varying outgassing rates (Figure 13). Most vents were located at the base of rocks which were slightly overhung, making them inaccessible to vertically-dropped probes. The three vents with the highest outgassing rates were capped with open pipes (55 mm diameter), and these were the focus of the tests as they presented a strong source of volcanic gas and a target which could be directly accessed from above.

Fig. 14   Flying over Shady Rest Fumarole near Mammoth Lakes, Inyo National Forest, CA

Shady Rest Fumarole (37.657683 N, 118.945091 W) was also trialled as a potential site for conducting testing with the UGCS (Figure 14). Very little activity was found at the site, with only a small amount of outgassing from a hole several metres away from the main rock peak. As such, testing at Shady Rest Fumarole focussed on operational procedures when over non-level ground with significant local terrain height changes.

1. Manual Data Collection

Both temperature and CO_2 measurements were taken by hand at Basalt Fumarole to establish an approximate 'control' data set to compare the UAV-gathered results with. Manually-gathered temperature readings of the capped vents were taken using a handheld Extech IR thermometer and matched well to those found in literature (97 °C measured, 92 °C from literature [24]). The fumaroles located at the base of rocks and in areas where noticeable outgassing from the ground was observed were also measured, typically falling somewhere between 65 °C and 90 °C. In areas where there was no apparent activity (such as the road), the ground temperature ranged from the ambient air temperature of around 10 °C in the shade up to 30 °C in areas of direct sunlight.

A hand placed in the gas escaping the capped fumaroles was used to qualitatively gauge the temperature reduction with distance from the opening. At around 50 mm from the opening, the gas was too hot to hold a hand near, however by 100 mm, only slight warmth was felt, and by 300 mm, there was no temperature difference between the fumarole gas and the ambient air. It was also observed that the outgassing rate was not consistent and fluctuated with a period of several seconds.

Fig. 15   Manually Sampling a Vent with the UGCS, Basalt Fumarole, Inyo National Forest, CA

The sample probe was placed by hand in one of the capped vents and CO_2 measurements were taken using the UGCS (Figure 15). Consistent measurements of the CO_2 readings were difficult to obtain, but measurements were always below the expected value of 97 % [24], typically falling between 60 % and 85 %. This is likely due to the CO_2 sensor not being calibrated for use at high altitudes, as well as the variable level of humidity entering the sensor and affecting the measurements. The silicone tube and probe survived the heat of the fumarole with no apparent damage, though significant condensation (that grew into water droplets) quickly formed inside the tube. While most components in the Gas Capture Module were able to handle the water, the condensation quickly caused the CO_2 sensor to fail. A spare CO_2 sensor was installed along with a makeshift water trap made from a 50 ml syringe, however the second sensor also failed, likely due to the incomplete removal of water by the water trap and residual water left inside the silicone tubing.

The condensed water also served as a medium to bring heat from the fumarole up through the silicone tubing and towards the more heat-sensitive Gas Capture Module. This transport of heat however was reasonably slow and it took several minutes of continuous pumping to raise the temperature of the tube at the UAV to levels that made it uncomfortable to hold.

2. Aerial Gas Sample Capture

Placing the probe in a fumarole from the air was significantly more difficult in the field, partly because of the smaller target (55 mm vs. 110 mm) and partly due to the uneven ground below the aircraft. A rangefinder provides feedback to

the flight controller on the distance to the ground, and using this, the flight controller attempts to maintain a set distance above the terrain. As *Volcano Drone* flies over rocks and undulations, it adjusts the altitude up and down in response, which in turn excites the probe sway. This effect was particularly pronounced at Shady Rest Fumarole. The features around Shady Rest Fumarole were very steep and caused the UAV to climb and descend quickly in response to the terrain. This made placing the probe in a specific location difficult as small lateral changes often would cause large altitude changes, exciting the probe sway.

Fig. 16   Capturing Gas from a Capped Fumarole at Basalt Fumarole

Back at Basalt Fumarole, the probe was placed inside a capped fumarole twice, and gas was successfully captured during one of these placements (Figure 16). The low density air (approximately 20 % lower than at sea level) affected the pump performance, and when coupled with the added friction from dust in the syringes, little gas was drawn into the sample canisters (15 ml in the field compared to 50 ml from lab testing). The amount of captured gas was not enough to pass back through the CO_2 sensor to get a reliable CO_2 measurement, and hence a direct comparison between the CO_2 levels in the gas captured from the UAV and the gas captured by hand could not be made.

3. Thermal Data from the UAV

Volcano Drone was manually piloted over the Basalt Fumarole area to collect thermal and RGB imagery using the on-board camera package. Images taken from low altitude showed distinct areas of heat, especially at the exits of the capped fumaroles (Figure 17). The measured temperatures of the capped fumaroles using the FLIR Lepton were typically around 85 °C, slightly lower than the 'control' measurements of 95 °C. This was most likely due the downwash of the UAV cooling to the fumarole, and the limited resolution of the FLIR averaging in some of the cooler surrounds. Around some rocks, large areas of heat were also detected, and similarly, matched reasonably well to the previously measured control values.

The RGB imagery showed little evidence that the area was thermally active, and many of the vents were either hidden under rocks or had significant shadows cast over them. Complementary visual information of the area (such as rock and soil types) however shows up well, aiding in the understanding of the terrain.

Imagery from higher altitudes above Basalt Fumarole show the benefits of using the FLIR to detect thermal activity over a wider area (Figure 18). While the low resolution of the FLIR Lepton limited the ability to identify the smaller, hotter individual vents (which blend into the rest of the terrain), Basalt Fumarole clearly stands out from the surrounding area. The higher temperature of local hotspots indicate potential sites to sample from, and this data could be used to generate flight paths in real time that capture samples from the hottest fumaroles as identified from the thermal imagery. When viewed in the visible spectrum of light, Basalt Fumarole appears much like the rest of the terrain, with no visible evidence of the area's thermal activity.
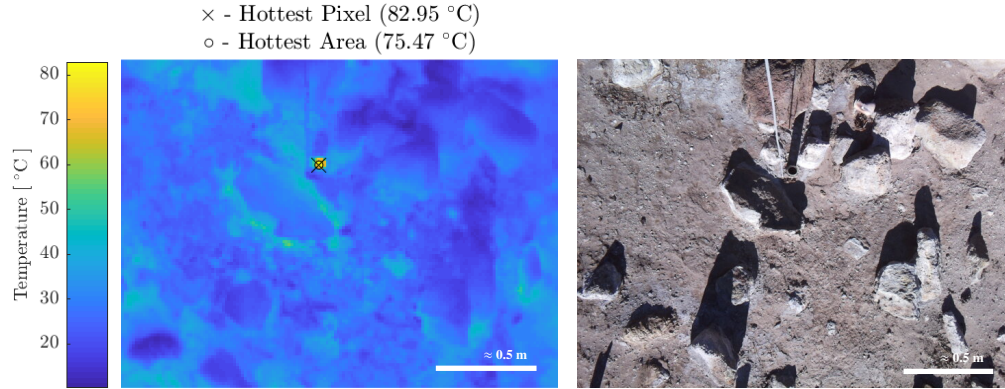
Fig. 17   One of the Vents at Basalt Fumarole as Captured by the Onboard FLIR (Long-Wave Thermal, Left) and RPi v2 (RGB, Right) Cameras from Approximately 2 m Altitude. The sample probe is deployed and the tube is visible at the top centre of the images.
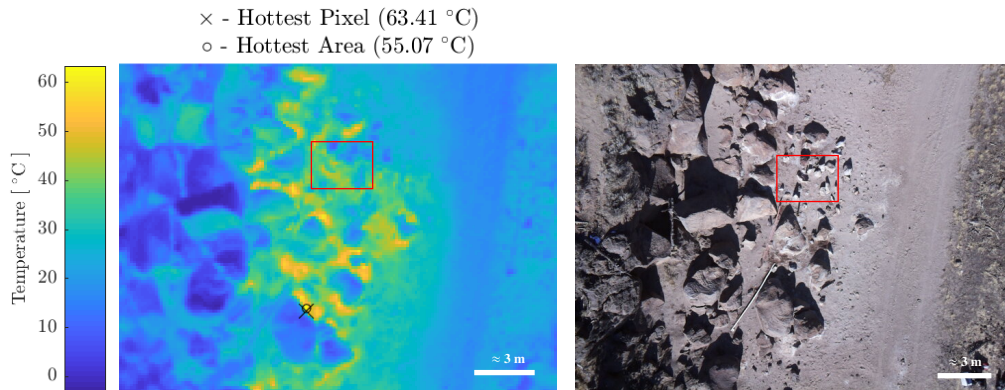

Fig. 18   Basalt Fumarole as Captured with the Onboard FLIR Lepton (Long-Wave Thermal, Left) and RPi v2 (RGB, Right) Cameras from Approximately 20 m Altitude. The thermally-active area is clearly visible and specific vents appear as small regions of higher temperatures. The region imaged in Figure 17 is marked by the red boxes. The smaller, hotter fumaroles are too small to be picked up by the FLIR and hence only the larger, cooler fumaroles stand out.

V. Future Work

A. Design for Harsh Environments and High Altitudes

Many elements of the UGCS succumbed to the high altitude and harsh environment of the Mammoth Lakes fumaroles. Future iterations will require a proper water trap and dehumidifying element (such as Nafion tube) to correctly condition the gas for the CO_2 sensor. Furthermore, improvements to the hardware such as a larger air pump to offset the loss of performance due to the lower air density will need to be implemented.

B. Sample Capture Methodology

While this paper proves the concept of remotely capturing gas samples from fumaroles using a UAV-borne gas capture system, the goal of collecting these samples at a high purity was not achieved due to the downwash of the UAV fouling the collected gas with ambient air. While it works for certain fumarole systems, placing the probe while in the air, landing, and waiting to capture the sample significantly reduces the number of fumaroles at which the presented system could operate, and hence an alternate solution will need to be developed. One potential solution would be to design an 'umbrella' which is deployed with the sample probe to protect the fumarole against the downwash of the UAV. The gases of the fumarole would then be allowed to re-concentrate before the gas was collected, giving a significantly less contaminated sample.

15

C. Fumarole Targetting

Targetting the small-diameter fumaroles manually was difficult, even for a well-practiced pilot. Developing a fumarole detection module and adding automatic guidance logic into the loop with the on-board autonomy package would greatly increase the efficiency at which the fumaroles could be targetted and sampled. Furthermore, these algorithms would not rely on *a priori* knowledge of the fumarole locations (as they are vision-based), and could be extended to include real-time path planning in un-mapped areas that are yet to be explored. This paper has shown that long-wave thermal imagery is a viable solution for detecting fumaroles that can be added in a light-weight package to a UAV, and that the thermal signature of a fumarole is both detectable and distinct from the surrounding terrain.

D. Active, Autonomous Probe Sway Damping

Probe sway both worsens the accuracy of the probe deployment and presents a significant hazard to the vehicle upon retraction. The location of the sample probe could be tracked in real-time using the feedback from the spool encoder and the RGB camera, enabling the high-level computer to know when it is safe to retract the probe. This could then be extended to actively move the UAV in a way to damp the sway of the probe end, reducing the effects of disturbances and removing the need to wait for the probe to naturally come to a rest in a steady state below the UAV.

VI. Conclusion

This paper has presented a novel, UAV-borne gas capture system that is capable of collecting gas samples from volcanic fumaroles. While the goal of capturing high-purity samples was not achieved due to the downwash of the UAV fouling the sample, significant advancements in the design and operation of such a system have been made. These advancements include a spool designed to deploy 2 m of silicone tube, a gas capture and storage system, and the ability to take *in situ* CO_2 measurements, all integrated into a single package which can interface with the host UAV. An in-development, light-weight autonomy package was also described and initial results of captured fumarole simulator imagery in both long-wave IR and RGB imagery were presented. Finally, the results of testing the system, both in a lab environment (indoors and outdoors) and in the field near Mammoth Lakes, CA, were presented, and represent a significant step towards autonomous, UAV-borne gas capture from fumaroles.

Acknowledgements

References

[1] Oppenheimer, C., Fischer, T., and Scaillet, B., "Volcanic Degassing: Process and Impact," *Treatise on Geochemistry*, Elsevier, 2014, pp. 111–179. https://doi.org/10.1016/b978-0-08-095975-7.00304-1.

[2] Broecker, W., "CO2: Earth's Climate Driver," *Geochemical Perspectives*, 2018, pp. 117–196. https://doi.org/10.7185/geochempersp.7.2.

[3] von Savigny, C., Timmreck, C., Buehler, S. A., Burrows, J. P., Giorgetta, M., Hegerl, G., Horvath, A., Hoshyaripour, G. A., Hoose, C., Quaas, J., Malinina, E., Rozanov, A., Schmidt, H., Thomason, L., Toohey, M., and Vogel, B., "The Research Unit VolImpact: Revisiting the volcanic impact on atmosphere and climate – preparations for the next big volcanic eruption," *Meteorologische Zeitschrift*, Vol. 29, No. 1, 2020, pp. 3–18. https://doi.org/10.1127/metz/2019/0999.

[4] Wong, K., Mason, E., Brune, S., East, M., Edmonds, M., and Zahirovic, S., "Deep Carbon Cycling Over the Past 200 Million Years: A Review of Fluxes in Different Tectonic Settings," *Frontiers in Earth Science*, Vol. 7, 2019. https://doi.org/10.3389/feart.2019.00263.

[5] Aiuppa, A., Fischer, T. P., Plank, T., and Bani, P., "CO2 Flux Emissions from the Earth's Most Actively Degassing Volcanoes, 2005–2015," *Scientific Reports*, Vol. 9, No. 1, 2019. https://doi.org/10.1038/s41598-019-41901-y.

[6] Robock, A., "Volcanic Eruptions and Climate," *Reviews of Geophysics*, Vol. 38, No. 2, 2000, pp. 191–219. https://doi.org/10.1029/1998rg000054.

[7] Aiuppa, A., Moretti, R., Federico, C., Giudice, G., Gurrieri, S., Liuzzo, M., Papale, P., Shinohara, H., and Valenza, M., "Forecasting Etna eruptions by real-time observation of volcanic gas composition," *Geology*, Vol. 35, No. 12, 2007, p. 1115. https://doi.org/10.1130/g24149a.1.

[8] D'Arcy, F., Stix, J., de Moor, J., Rüdiger, J., Diaz, J., Alan, A., and Corrales, E., "Drones Swoop in to Measure Gas Belched from Volcanoes," *Eos*, Vol. 99, 2018. https://doi.org/10.1029/2018eo102329.

[9] Burton, M. R., Sawyer, G. M., and Granieri, D., "Deep Carbon Emissions from Volcanoes," *Reviews in Mineralogy and Geochemistry*, Vol. 75, No. 1, 2013, pp. 323–354. https://doi.org/10.2138/rmg.2013.75.11.

[10] James, M., Carr, B., D'Arcy, F., Diefenbach, A., Dietterich, H., Fornaciai, A., Lev, E., Liu, E., Pieri, D., Rodgers, M., Smets, B., Terada, A., von Aulock, F., Walter, T., Wood, K., and Zorn, E., "Volcanological Applications of Unoccupied Aircraft Systems (UAS): Developments, strategies, and future challenges," *Volcanica*, 2020, pp. 67–114. https://doi.org/10.30909/vol.03.01.67114.

[11] McGonigle, A. J. S., Aiuppa, A., Giudice, G., Tamburello, G., Hodson, A. J., and Gurrieri, S., "Unmanned aerial vehicle measurements of volcanic carbon dioxide fluxes," *Geophysical Research Letters*, Vol. 35, No. 6, 2008. https://doi.org/10.1029/2007gl032508.

[12] Mori, T., Hashimoto, T., Terada, A., Yoshimoto, M., Kazahaya, R., Shinohara, H., and Tanaka, R., "Volcanic Plume Measurements Using a UAV for the 2014 Mt. Ontake Eruption," *Earth, Planets and Space*, Vol. 68, No. 1, 2016. https://doi.org/10.1186/s40623-016-0418-0.

[13] Rüdiger, J., Tirpitz, J.-L., de Moor, J. M., Bobrowski, N., Gutmann, A., Liuzzo, M., Ibarra, M., and Hoffmann, T., "Implementation of Electrochemical, Optical and Denuder-Based Sensors and Sampling Techniques on UAV for Volcanic Gas Measurements: Examples from Masaya, Turrialba and Stromboli volcanoes," *Atmospheric Measurement Techniques*, Vol. 11, No. 4, 2018, pp. 2441–2457. https://doi.org/10.5194/amt-11-2441-2018.

[14] Liu, E. J., Wood, K., Mason, E., Edmonds, M., Aiuppa, A., Giudice, G., Bitetto, M., Francofonte, V., Burrow, S., Richardson, T., Watson, M., Pering, T. D., Wilkes, T. C., McGonigle, A. J. S., Velasquez, G., Melgarejo, C., and Bucarey, C., "Dynamics of Outgassing and Plume Transport Revealed by Proximal Unmanned Aerial System (UAS) Measurements at Volcán Villarrica, Chile," *Geochemistry, Geophysics, Geosystems*, Vol. 20, No. 2, 2019, pp. 730–750. https://doi.org/10.1029/2018gc007692.

[15] Schellenberg, B., Richardson, T., Richards, A., Clarke, R., and Watson, M., "On-Board Real-Time Trajectory Planning for Fixed Wing Unmanned Aerial Vehicles in Extreme Environments," *Sensors*, Vol. 19, No. 19, 2019, p. 4085. https://doi.org/10.3390/s19194085.

[16] Wood, K., Liu, E. J., Richardson, T., Clarke, R., Freer, J., Aiuppa, A., Giudice, G., Bitetto, M., Mulina, K., and Itikarai, I., "BVLOS UAS Operations in Highly-Turbulent Volcanic Plumes," *Frontiers in Robotics and AI*, Vol. 7, 2020. https://doi.org/10.3389/frobt.2020.549716.

[17] Li, C., Han, W., Peng, M., Zhang, M., Yao, X., Liu, W., and Wang, T., "An Unmanned Aerial Vehicle-Based Gas Sampling System for Analyzing CO2 and Atmospheric Particulate Matter in Laboratory," *Sensors*, Vol. 20, No. 4, 2020, p. 1051. https://doi.org/10.3390/s20041051.

[18] ArduPilot, "ArduPilot: Trusted, Versatile, Open," https://ardupilot.org/, n.d.

[19] Lynch, D. K., Hudnut, K. W., and Adams, P. M., "Development and Growth of Recently-Exposed Fumarole Fields near Mullet Island, Imperial County, California," *Geomorphology*, Vol. 195, 2013, pp. 27–44. https://doi.org/10.1016/j.geomorph.2013.04.022.

[20] Casadevall, T. J., and Hazlett, R. W., "Thermal areas on Kilauea and Mauna Loa Volcanoes, Hawaii," *Journal of Volcanology and Geothermal Research*, Vol. 16, No. 3-4, 1983, pp. 173–188. https://doi.org/10.1016/0377-0273(83)90028-8.

[21] Zelenski, M., and Taran, Y., "Geochemistry of Volcanic and Hydrothermal Gases of Mutnovsky Volcano, Kamchatka: Evidence for mantle, slab and atmosphere contributions to fluids of a typical arc volcano," *Bulletin of Volcanology*, Vol. 73, No. 4, 2011, pp. 373–394. https://doi.org/10.1007/s00445-011-0449-0.

[22] Corrsin, S., and Uberoi, M. S., "Further Experiments on the Flow and Heat Transfer in a Heated Turbulent Air Jet," Tech. rep., jan 1950. URL https://ntrs.nasa.gov/search.jsp?R=19930092055.

[23] Mazzini, A., Svensen, H., Etiope, G., Onderdonk, N., and Banks, D., "Fluid Origin, Gas Fluxes and Plumbing System in the Sediment-Hosted Salton Sea Geothermal System (California, USA)," *Journal of Volcanology and Geothermal Research*, Vol. 205, No. 3-4, 2011, pp. 67–83. https://doi.org/10.1016/j.jvolgeores.2011.05.008.

[24] Bergfeld, D., Vaughan, R. G., Evans, W. C., and Olsen, E., "Monitoring Ground-Surface Heating During Expansion of the Casa Diablo Production Well Field at Mammoth Lakes, California," *Geothermal Resources Council Transactions*, Vol. 39, 2015.

[25] IsoTech Labs, "IsoTubes," http://www.isotechlabs.com/products/isotubes/, Last Accessed: Nov 2020.

[26] Eby, P., Gibson, J. J., and Yi, Y., "Suitability of selected free-gas and dissolved-gas sampling containers for carbon isotopic analysis," *Rapid Communications in Mass Spectrometry*, Vol. 29, No. 13, 2015, pp. 1215–1226. https://doi.org/https://doi.org/10.1002/rcm.7213.

[27] Zorn, E. U., Walter, T. R., Johnson, J. B., and Mania, R., "UAS-Based Tracking of the Santiaguito Lava Dome, Guatemala," *Scientific Reports*, Vol. 10, No. 1, 2020. https://doi.org/10.1038/s41598-020-65386-2.

[28] mavlink, "MAVLink Developer Guide," https://mavlink.io/en/, n.d.